C.2a.1.24-Methyl orange dye removal using NiFe-NO3 and.pdf

By Risfidian Mohadi

WORD COUNT 2952
TIME SUBMITTED 22-JAN-2022 11:08AM
PAPER ID 81673338

Methyl orange dye removal using Ni/Fe-NO_3 and Ni/Fe-[α-$SiW_{12}O_{40}$] layered double hydroxides

Methyl orange dye removal using Ni/Fe-NO_3 and Ni/Fe-[α-$SiW_{12}O_{40}$] layered double hydroxides

A Lesbani[1, 2], T Taher[2, 3], N R Palapa[3], R Mohadi[2, 3], A Yuliana[3] and Mardiyanto[4]

[1]Graduate School of Mathematics and Natural Sciences, Faculty of Mathematics and Natural Sciences (FMIPA), Universitas Sriwijaya, Ogan Ilir 30662, Indonesia
[2]Research Centre of Inorganic Materials and Coordination Complexes, Faculty of Mathematics and Natural Sciences, Universitas Sriwijaya, Ogan Ilir 30662, Indonesia
[3]Department of Chemistry, Faculty of Mathematics and Natural Sciences (FMIPA), Universitas Sriwijaya, Ogan Ilir 30662, Indonesia
[4]Department of Pharmacy, Faculty of Mathematics and Natural Sciences (FMIPA), Universitas Sriwijaya, Ogan Ilir 30662, Indonesia

Corresponding author's email: aldeslesbani@pps.unsri.c.id

Abstract. The material of layered double hydroxide (LDH) Ni/Fe-NO_3 was prepared by coprecipitation method under basic condition. Ni/Fe LDH was modified by intercalation using K_4[α-$SiW_{12}O_{40}$] to form Ni/Fe-[α-$SiW_{12}O_{40}$]. All materials were characterized by X-ray and FTIR spectroscopy. Ni/Fe LDH and intercalated Ni/Fe LDH were used as adsorbent of methyl orange dye from the aqueous solution. The parameter of adsorption such as kinetic and also thermodynamic adsorption of methyl orange on LDHs were investigated. X-Ray analysis showed that the diffraction at 11.53° [003] of Ni/Fe-NO_3 has interlayer distance 7.67 Å shift to 8.20° [003] of Ni/Fe-[α-$SiW_{12}O_{40}$] with interlayer distance 10.78 Å. FTIR spectra of Ni/Fe-NO_3 and Ni/Fe-[α-$SiW_{12}O_{40}$] show the wavenumber at 1600 cm^{-1} due to vibration of LDHs anion. Adsorption of methyl orange onto Ni/Fe-NO_3 and Ni/Fe-[α-$SiW_{12}O_{40}$] follow the pseudo second-order kinetic model, where intercalated material has a higher reactivity than Ni/Fe-NO_3 before intercalation. Isotherm model Freundlich was more fitted than isotherm Langmuir for the adsorption of methyl orange on LDHs with multilayer physical adsorption process. Adsorption capacity of methyl orange on Ni/Fe-[α-$SiW_{12}O_{40}$] as adsorbent was slightly higher (up to 7.226 $mg.g^{-1}$) than Ni/Fe-NO_3 as adsorbent (3.190 $mg.g^{-1}$).

Keywords: Layered double hydroxide, Ni/Fe, K_4[α-$SiW_{12}O_{40}$], methyl orange, adsorption

1. Introduction

The research of dyes treatment from wastewater has been conducted until this decade. Various procedures have been used to eliminate dyes from wastewater, namely coagulation [1], filtration [2], and also adsorption [3]. Adsorption is a reliable method due to the high efficiency, simple, and ease of operation. The successful adsorption process depends on properties of adsorbent. Wide range of adsorbents have been synthesized to remove dyes from wastewater such as bentonite [4], kaolinite [5], zeolite [6], and also layered double hydroxide [7]. Layered double hydroxide (LDH) is anionic layered structure material, which has empirical common formula of $[M^{2+}(1-x)M^{3+}x(OH)_2](A^{n-})x/nH_2O$. LDH

has positively charged and exchangeable anion in the interlayer [8]. The structure of LDH has a unique structure due to anion exchange properties to form selective structure for application of LDH. However, the distance of basal spacing of layered materials still has small interlayer constraints and narrow layer spacing due to the small exchange ions such as nitrate, carbonate, sulfate, and chloride thus layered double hydroxides need to be modified to increase its interlayer distance [9].

Adsorption of congo red dye from aqueous solution was conducted using Mg-Al-layered double hydroxide as adsorbent. The adsorption process was controlled mainly by electrostatic interaction [10]. Anionic dye such as congo red was also removed by Mg-Fe-CO_3 as adsorbent by reusing the adsorbent of Mg-Fe-CO_3 layered double hydroxide for several times [11]. The adsorption of methyl orange, which is an anionic dye was also carried out using Mg-Al layered double hydroxide as adsorbent with 3D structure with high adsorption capacity [12]. Intercalated layered double hydroxide with heteropoly blue compound $[PW_{10}Mo_2O_{40}]^{5-}$ showed an ability for cationic dye removal such as methylene blue [13]. The intercalated layered double hydroxide showed a higher adsorption capacity of methylene blue than the pure layered double hydroxide. Thus, the research of intercalated layer double hydroxide with polyoxometalate is an interesting top for removal of dyes from aqueous solution.

In this research, Ni/Fe-NO_3 was intercalated with Keggin ion $[\alpha\text{-}SiW_{12}O_{40}]^{4-}$ to form Ni/Fe-[α-$SiW_{12}O_{40}$] LDH. Keggin ion is used due to the stability of this polyoxometalate and easy to synthesize in acid aqueous medium. Materials were characterized using X-ray and FTIR analyses. The pHpzc of materials were also identified. Then materials were used as adsorbent of methyl orange from aqueous solution. Factors that influence the adsorption process such as adsorption time, concentration of methyl orange, and adsorption temperature were studied in this research to obtain the kinetic and thermodynamic parameters of adsorption.

2. Materials and method

2.1. Chemicals and instrumentation

Chemicals were supplied from Merck and Sigma Aldrich as follows nickel(II) nitrate, iron(III) nitrate, sodium tungsten, sodium carbonate, sodium metasilicate, hydrochloric acid and sodium chloride. Keggin ion of $[\alpha\text{-}SiW_{12}O_{40}]^{4-}$ was synthesized according to the literature [XX]. Water was supplied from Research Center of Inorganic Materials and Coordination Complexes, Universitas Sriwijaya. X-ray analysis was measured by Rigaku Miniflex-600 X-ray powder diffraction. Sample was scanned at scan speed 1 deg min^{-1}. FTIR spectra were obtained using Shimadzu FTIR Prestige-21 and spectra were recorded at wavenumber 400–4000 cm^{-1}. Analysis of methyl orange dye was performed using UV-Vis BioBase BK-UV 1800 PC spectrophotometer.

2.2. Synthesis of material Ni/Fe-NO_3 and Ni/Fe-[α-$SiW_{12}O_{40}$]

Synthesis of Ni/Fe-NO_3 LDH was conducted using coprecipitation method according to Yang et al. [14] with slight modification. Nickel(II) nitrate was dissolved with water to form 0.3 M $Ni(NO_3)_2$. Solution of nickel nitrate was mixed with solution of iron(III) nitrate 0.1 M to form solution A. Sodium hydroxide 2 M was mixed with solution of sodium carbonate 1 M to form solution B. Solution A was mixed with solution B by slowly stirring at room temperature. The solution mixture was adjusted to pH 10–11 by the addition of sodium hydroxide solution. The solid material was formed under constant stirring. Solid material was dried for 24 h to obtain Ni/Fe-NO_3 LDH. Material Ni/Fe-NO_3 LDH is intercalated with Keggin ion to form Ni/Fe-[α-$SiW_{12}O_{40}$] using ion exchange method. Compound $K_4[\alpha\text{-}SiW_{12}O_{40}]$ was dissolved with water (solution A). Ni/Fe-NO_3 LDH was mixed with solution of sodium hydroxide (solution B). The solution was introduced with nitrogen gas then the solution A was mixed with solution B under nitrogen condition. The temperature of mixture was adjusted at 40 °C for 24 h to obtain solid material of Ni/Fe-[α-$SiW_{12}O_{40}$].

2.3. pH point zero charge (pzc) and adsorption experiments

Analysis of pHpzc was conducted using aqueous solution of sodium hydroxide or hydrochloric acid. A series of solution sodium chloride was adjusted to pH 1–10 using aqueous solution of sodium hydroxide or aqueous solution of hydrochloric acid. Then, LDH was added to the solution series. The solutions series was stirred for 24 h. The solution's pH after filtration was determined using pH meter. pHpzc graph was created by plotting the initial versus final pH.

The adsorption of methyl orange was performed under pHpzc using Ni/Fe-NO_3 and Ni/Fe-[α-$SiW_{12}O_{40}$] as adsorbents. Adsorption was studied by investigation of adsorption time, initial concentration of methyl orange and adsorption temperature. Adsorption time was varied at 5–120 min. Concentration of methyl orange was varied from 10–30 mg L^{-1} at temperature 35, 40, 45 and 50 °C.

3. Results and discussion

Materials Ni/Fe-NO_3 and Ni/Fe-[α-$SiW_{12}O_{40}$] LDHs were analyzed using X-ray analysis and the patterns are shown in figure 1. Material Ni/Fe-NO_3 has diffraction pattern at 11.53° (003), 23.06° (006), 34.83° (012), 39.70° (015) and 60.54° (110) [15]. The formation of well-ordered layer material was identified at 11.53° (003) resulting the interlayer distance of 7.67Å. Material Ni/Fe-NO_3 was intercalated with anion $[\alpha\text{-}SiW_{12}O_{40}]^{4-}$ to form Ni/Fe-[α-$SiW_{12}O_{40}$]. Ni/Fe-[α-$SiW_{12}O_{40}$] has the diffraction pattern at 8.20° (003), 11°, 15–20°, 22–25°, 35–40° and 59–60°. Diffraction at (003) was shifted to a lower angle due to the insertion of Keggin ion. Interlayer distance at 8.20° (003) was 10.78 Å. The interlayer distance after intercalation was increased to 3.11 Å.

The Ni/Fe-NO_3 and Ni/Fe-[α-$SiW_{12}O_{40}$] LDH FTIR spectra are shown in figure 2a and figure 2b. Material Ni/Fe-NO_3 has vibration at 3400 cm^{-1} (ν OH), 3000 cm^{-1} (ν OH) and 1300 cm^{-1} [16]. The unique vibration at 1300 cm^{-1} was assigned to nitrate vibration. Nitrate ion was located on the interlayer distance on LDH. Intercalated material Ni/Fe-[α-$SiW_{12}O_{40}$] has similar main vibrations with Ni/Fe-NO_3. The intensity of vibration at 1300 cm^{-1} was decreased due to the insertion of Keggin ion $[\alpha\text{-}SiW_{12}O_{40}]^{4-}$ on interlayer Ni/Fe LDH. Vibrations at 700–900, 1100 cm^{-1} on Ni/Fe-[α-$SiW_{12}O_{40}$] were attributed to W-O-W, W=O, and Si-O vibrations of Keggin ion.

Figure 3 shows that intersection point of Ni/Fe-NO_3 LDH was at 7 while Ni/Fe-[α-$SiW_{12}O_{40}$] at 9. There is no charges at that intersection point and charges of materials were zero. pHpzc below the intersection point is dominated by proton and material with positive charge. On the other hand, negative charge was dominated at above intersection point of pHpzc due to hydroxyl ion form solution. Adsorption of methyl orange on Ni/Fe-NO_3 and Ni/Fe-[α-$SiW_{12}O_{40}$] LDHs was conducted at pHpzc.

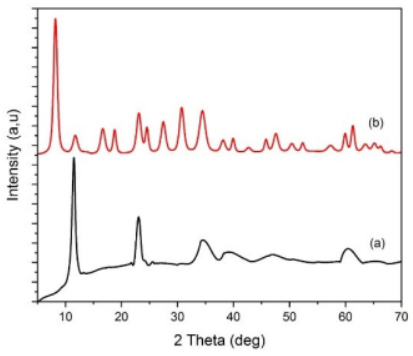

Figure 1. XRD powder pattern of Ni/Fe-NO_3 (a) and Ni/Fe-[α-$SiW_{12}O_{40}$] (b) LDHs.

Adsorption of methyl orange on Ni/Fe-NO_3 and Ni/Fe-[α-$SiW_{12}O_{40}$] LDHs was studied by investigating the adsorption time, concentration of methyl orange and adsorption temperature. Effect of adsorption time of congo red on both Ni/Fe-NO_3 and Ni/Fe-[α-$SiW_{12}O_{40}$] LDHs is shown in figure 4.

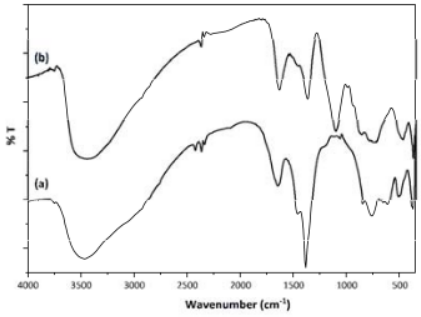

Figure 2. FTIR spectra of Ni/Fe-NO_3 (a) and Ni/Fe-[α-$SiW_{12}O_{40}$] (b) LDHs.

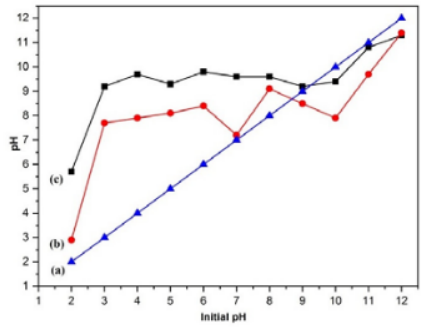

Figure 3. pHpzc graph of initial pH (a), Ni/Fe-NO_3 (b,) and Ni/Fe-[α-$SiW_{12}O_{40}$] (c) LDHs.

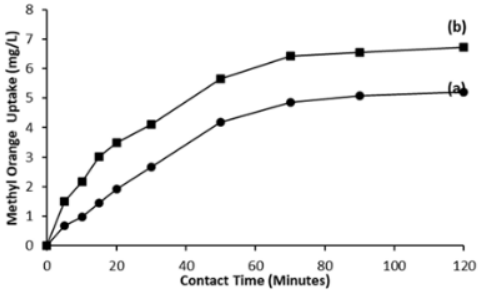

Figure 4. Effect adsorption time of Ni/Fe-NO_3 (a) Ni/Fe-[α-$SiW_{12}O_{40}$] and (b) LDHs.

Adsorption of methyl orange for both LDHs increases with the increase of adsorption time and reached the equilibrium at 70 min for both LDHs. The pattern of methyl orange adsorption on both LDHs was similar but the amount of adsorption was different. The adsorbent Ni/Fe-[α-$SiW_{12}O_{40}$] has a higher adsorption amount than Ni/Fe-NO_3. Data of adsorption time in figure 4 was processed using the pseudo first and second order kinetic models to obtain kinetic adsorption rate for methyl orange on LDH [17].

The data of kinetic model as shown in table 1 showed that methyl orange was adsorbed on both of Ni/Fe-NO_3 and Ni/Fe-[α-$SiW_{12}O_{40}$] LDHs by following the pseudo second-order kinetic model. Adsorption rate for Ni/Fe-[α-$SiW_{12}O_{40}$] was faster than Ni/Fe-NO_3 thus, the adsorbent Ni/Fe-[α-$SiW_{12}O_{40}$] has a higher reactivity than adsorbent Ni/Fe-NO_3.

The effect of methyl orange concentration and temperature adsorption on Ni/Fe-NO_3 and Ni/Fe-[α-$SiW_{12}O_{40}$] LDHs is shown in figure 5. Adsorption of methyl orange was increased with the increase of methyl orange concentration for both LDHs. The increase adsorption temperature was also increasing the adsorption amount of methyl orange. The data in figure 5 showed that adsorption of methyl orange on LDHs was a multilayer process, which was indicated at concentration 20 mg L^{-1} for both LDHs. Thermodynamic adsorption parameter of methyl orange can be obtained using the data in figure 5, which was calculated using thermodynamic equation [18]. The thermodynamic data is presented in table 2.

The data in table 2 showed the value of adsorption capacity, Gibbs energy, enthalpy, and entropy of methyl orange adsorption on LDHs. The adsorption capacity of methyl orange for both adsorbents in the range 3.190–7.226 mg g^{-1} showed an increase of adsorption capacity after intercalated Ni/Fe-NO_3

Table 1. Kinetic model of methyl orange adsorption.

Kinetic model	Value	Adsorbent	
		Ni/Fe	Ni/Fe-[α-$SiW_{12}O_{40}$]
Pseudo first-order kinetic model	Qe exp (mg g^{-1})	2.086	2.686
	Qe calc (mg g^{-1})	1.633	1.774
	R^2	0.429	0.446
Pseudo second-order kinetic model	Qe exp (mg g^{-1})	2.086	2.686
	Qe calc (mg g^{-1})	0.008	0.017
	R^2	0.831	0.964

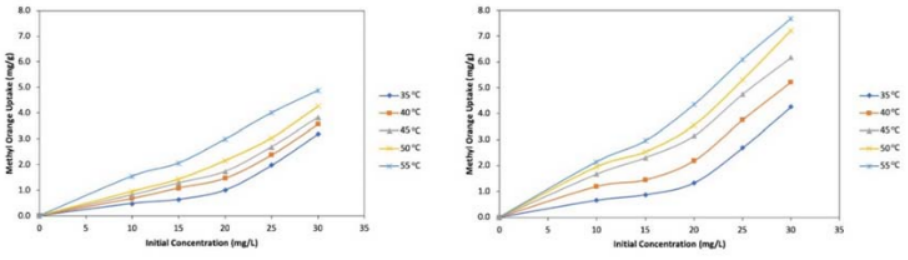

(a) (b)

Figure 5. Effect of methyl orange concentration and temperature adsorption on Ni/Fe-NO_3 (a) Ni/Fe-[α-$SiW_{12}O_{40}$] and (b) LDHs.

Table 2. Thermodynamic adsorption parameter of methyl orange on LDH.

LDHs	T (°C)	Q_e (mg g^{-1})	$\Delta G°$ (kJ.mol^{-1})	$\Delta H°$ (kJ.mol^{-1})	$\Delta S°$ (J.mol^{-1}.K^{-1})
Ni/Fe-NO_3	35	3.190	-20.693	25.707	67.269
	40	3.564	-21.055		
	45	3.826	-21.391		
	50	4.256	-21.728		
Ni/Fe-[α-$SiW_{12}O_{40}$]	35	4.256	-47.117	50.998	153.144
	40	5.221	-47.934		
	45	6.169	-48.700		
	50	7.226	-49.465		

to Ni/Fe-[α-$SiW_{12}O_{40}$]. All adsorption of methyl orange on LDHs was spontaneously occurred due to the negative value of Gibbs energy. Adsorption of methyl orange on LDH was classified as physical adsorption with energy in the range 25.707–50.998 kJ mol^{-1} and also there was a randomness increase of adsorption system on Ni/Fe-[α-$SiW_{12}O_{40}$] as adsorbent.

4. Conclusion

Adsorption of methyl orange on Ni/Fe-NO_3 and Ni/Fe-[α-$SiW_{12}O_{40}$] follows the kinetic pseudo second-order model with high reactivity of Ni/Fe-[α-$SiW_{12}O_{40}$]. Adsorption capacity of methyl orange on Ni/Fe-[α-$SiW_{12}O_{40}$] (up to 7.226 mg g^{-1}) was higher than Ni/Fe-NO_3 (up to 4.256 mg g^{-1}) and adsorption was categorized as physical adsorption with the energy range of 25.707–50.998 kJ mol^{-1}. The adsorption process was spontaneously occurred by the increase of randomness system from Ni/Fe-NO_3 to Ni/Fe-[α-$SiW_{12}O_{40}$].

Acknowledgment

Authors thank to Ministry of Research, Technology and Higher Education, Republic Indonesia for supporting this research through "High Penelitian Dasar (PD)" contract number 0057.10/UN9/SB3.LP2M.PT/2019 and also to Research Center of Inorganic Materials and Coordination Complexes, Faculty of Mathematics and Natural Sciences, Universitas Sriwijaya for research facilities.

References

[1] Li H, Liu S, Zhao J and Feng N 2016 *Colloid. Surf. A Physicochem. Eng. Asp.* **494** 222-7
[2] Ong P J, Tay S W and Hong L 2018 *J. Environ. Chem. Eng.* **6** 4612-22
[3] Clark I, Smith J, Gomes R L and Lester E 2019 *J. Environ. Chem. Eng.* **7** 103175
[4] Taher T, Rohendi D, Mohadi R and Lesbani A 2018 *Chiang Mai J. Sci.* **45** 1770-81
[5] Kamel M M, Youssef B M and Kamel M M 1991 *Dyes Pigm.* **15** 175-82
[6] Alver E and Metin A Ü 2012 *Chem. Eng. J.* **200-202** 59-67
[7] Palapa N R, Mohadi R and Lesbani A 2018 *AIP Conf. Proc.* **2026** 020018
[8] Taher T et al. 2019 *Indones. J. Chem.* **19** 873-81
[9] Shafigh M, Hamidpour M and Furrer G 2019 *Appl. Clay Sci.* **170** 135-42
[10] Lafi R, Charradi K, Djebbi M A, Amara A B H and Hafiane A 2016 *Adv. Powder Technol.* **27** 232-7
[11] Ahmed I M and Gasser M S 2012 *Appl. Surf. Sci.* **259** 650-6
[12] Cao Y et al. 2019 *Mater. Lett.* **257** 126695

[13] Bi B, Xu L, Xu B and Liu X 2011 *Appl. Clay Sci.* **54** 242-7
[14] Yang Y J and Li W 2018 *J. Electroanal. Chem.* **823** 499-504
[15] Zhan T et al. 2019 *J. Colloid Interf. Sci.* **552** 671-7
[16] Khataee A et al. 2019 *Chem. Eng. J.* **375** 122102
[17] Taher T et al. 2018 *AIP Conf. Proc.* **2049** 020011
[18] Taher T, Rohendi D, Mohadi R and Lesbani A 2019 *Arab J. Basic Appl. Sci.* **26** 125-36

C.2a.1.24-Methyl orange dye removal using NiFe-NO3 and.pdf

ORIGINALITY REPORT

20%
SIMILARITY INDEX

PRIMARY SOURCES

1	repository.uin-malang.ac.id Internet	108 words — 4%
2	ejournal2.undip.ac.id Internet	91 words — 3%
3	journal.ugm.ac.id Internet	85 words — 3%
4	gfzpublic.gfz-potsdam.de Internet	50 words — 2%
5	unsri.portalgaruda.org Internet	40 words — 1%
6	dns2.asia.edu.tw Internet	36 words — 1%
7	pdfs.semanticscholar.org Internet	36 words — 1%
8	link.springer.com Internet	24 words — 1%
9	jestec.taylors.edu.my Internet	19 words — 1%

10	jhhhm.halal.ac.ir Internet	19 words — 1%
11	onlinelibrary.wiley.com Internet	17 words — 1%
12	univoak.eu Internet	17 words — 1%
13	Www.intechopen.com Internet	16 words — 1%

EXCLUDE QUOTES	OFF	EXCLUDE MATCHES	< 1%
EXCLUDE BIBLIOGRAPHY	ON		